Observation of Beta and X Rays with 3-D-Architecture Silicon Microstrip Sensors

Christopher J. Kenney, Sherwood I. Parker, Brad Krieger, Bernhard Ludewigt, Tim P. Dubbs, and Hartmut Sadrozinski

***Abstract*—The first silicon radiation sensors based on the three-dimensional (3-D) architecture have been successfully fabricated. X-ray spectra from Iron-55 and Americium-241 have been recorded by reading out a 3-D architecture detector via wire bonds to a low-noise, charge-sensitive preamplifier. Using a beta source, coincidences between a 3-D sensor and a plastic scintillator were observed. This is the first observation of ionizing radiation using a silicon sensor based on the 3-D architecture. Details of the apparatus and measurements are described.**

***Index Terms*—Radiation detectors, radiation sensors, semiconductor detectors, semiconductor sensors, silicon sensors, three-dimensional, 3-D sensors, (3-D) silicon sensors.**

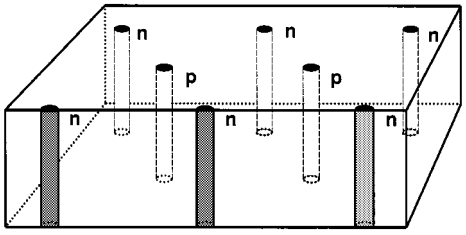

Fig. 1. Schematic, 3-D view of part of a sensor with 3-D electrodes penetrating through the substrate. The front border of the figure is drawn through the center of three electrodes.

I. Introduction

THE three-dimensional (3-D) architecture for radiation sensors has electrodes that are perpendicular to the wafer's surface, and extend partially or completely through the three-dimensional volume of the wafer. This is in contrast to radiation sensors built using planar technology where the electrode structures are parallel to the surface and restricted to be within a few microns of the wafer's top and bottom surfaces. Fig. 1 shows a schematic view of part of such a sensor, with the front surface in the drawing cut through the middle of three n-type electrodes that penetrate all the way from the top surface to the bottom. Both planar and 3-D silicon sensors use reverse-biased p-i-n diodes, but the electric field in the former is largely perpendicular to the surfaces, while in 3-D sensors, it is parallel. Details on how these devices were fabricated as well as simulations can be found in earlier publications [1]–[3].

There are several properties of planar-architecture radiation sensors that can be improved upon by the incorporation of a 3-D or nonplanar architecture. Among them are the following.

1) At high fluences of interacting particles, radiation damage to the silicon crystal produces damage centers that, in depleted silicon, are charged, increasing the voltage required to fully deplete a silicon p-i-n detector [4]. By allowing the spacing between N and P type electrodes, and hence the depletion distance, to be less than the wafer's thickness, 3-D architecture sensors can be fully depleted after higher fluences than standard planar-architecture sensors [5].
2) Charged particles usually come in parallel to the electrodes, and so all the ionization approaches the electrode, where the induced signal is largest, at nearly the same time. This combined with the short interelectrode distance, produces a large pulse with a fast rise-time.
3) For materials, such as GaAs and diamond, which have significant charge trapping and hence poor charge collection efficiency, the use of a 3-D architecture can reduce the drift path of the signal carriers and hence produce a higher signal-to-noise ratio [6].
4) The addition of active edges [3] should allow the fabrication of sensors with negligible dead volume at the die edges and the seamless tiling of large areas with butted or overlapping sensors.

Earlier results using a pulsed infrared light source [3] indicated that 3-D sensors did deplete at low, reverse-bias voltages as expected. Radioactive sources emitting X rays and gamma rays were then used in this study to demonstrate the ability of the 3-D silicon sensors to detect ionizing radiation. Results of these X-ray measurements and the methods used to achieve them are detailed in the following sections.

II. Measurements with X and Gamma Rays

The geometry of the sensor used for these measurements was that of a strip detector where sets of twelve, like-type electrodes were tied together to form line segments. Each individual electrode extended completely through the wafer and consisted of a doped polycrystalline silicon core from which dopant atoms have been diffused into the surrounding single-crystal silicon. The separation between electrodes within a strip was 100 μm, and that between neighboring strips of opposite type was also 100 μm. The n-type strips alternated with p-type strips in an interdigitated arrangement, with the n-type electrodes midway between the p-type electrodes in the strip direction. Surrounding

Manuscript received August 16, 2000; revised December 18, 2000. This work was supported in part by the U.S. Department of Energy under Grant DE-FG03-94ER40833 and in part by the Stanford Nanofabrication Facility by the National Science Foundation.

C. J. Kenney and S. I. Parker are with the University of Hawaii, Honolulu, HI 96822 USA.

B. Krieger and B. Ludewigt are with Lawrence Berkeley National Laboratory, Berkeley, CA 94720 USA.

T. P. Dubbs and H. Sadrozinski is with the University of California at Santa Cruz, Santa Cruz, CA 95064 USA.

Publisher Item Identifier S 0018-9499(01)02580-1.

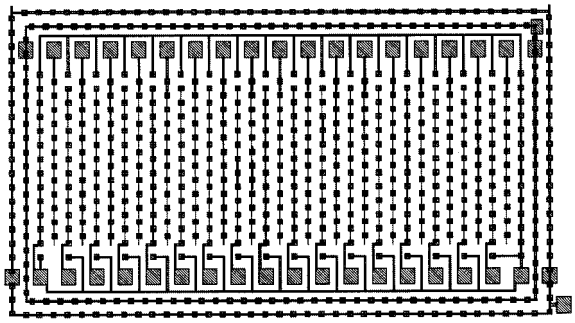

Fig. 2. Layout of a 3-D microstrip sensor. The interdigitated strips alternate between n type and p type.

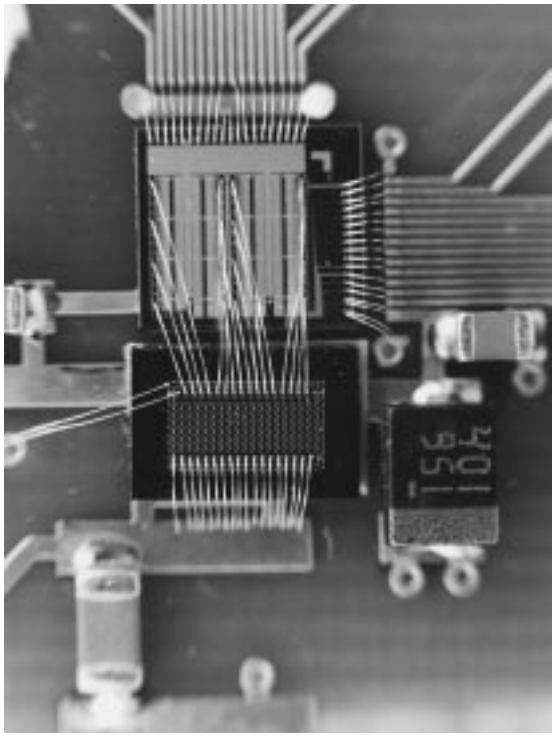

Fig. 3. Photograph of the 3-D sensor on the left, wire-bonded to the read-out circuit on the right.

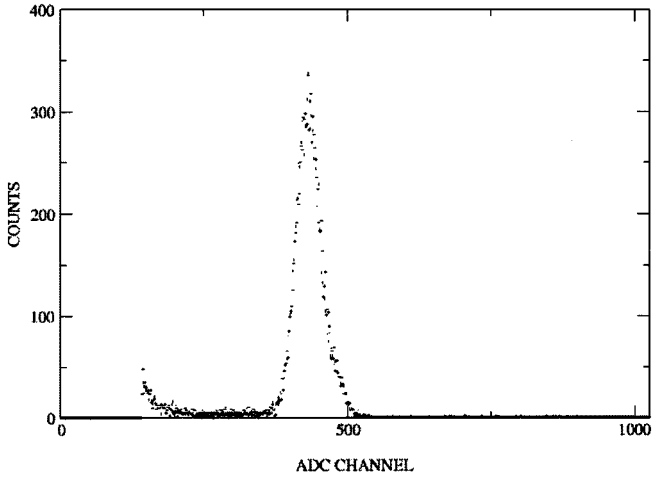

Fig. 4. Spectrum from an Iron-55 source.

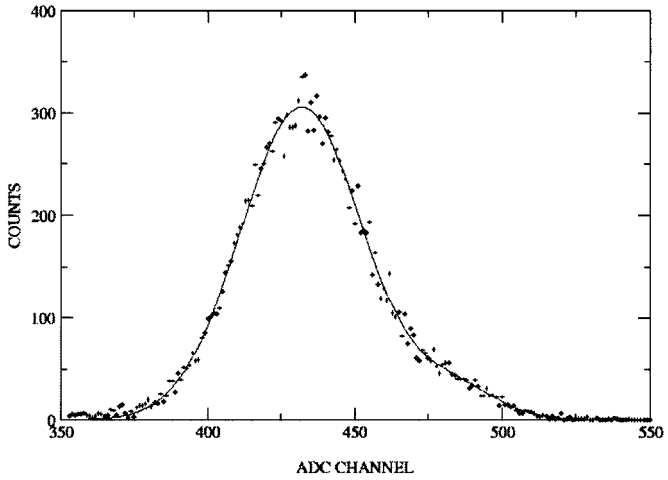

Fig. 5. Fit to the Manganese K_α/K_β peaks using two Gaussians with a common best-fit FWHM of 652 eV. Taken at room temperature with an Iron-55 source.

the strips are three concentric guard fences each composed of a set of electrodes tied together with an aluminum bus. The middle of the three fences used n-type electrodes, while the outer and inner guard fences used p-type electrodes. For these measurements the 121-μm-thick sensor was left fusion bonded to a 525-μm-thick support wafer [3]. A layout of the 3-D strip sensor is shown in Fig. 2.

Each of the 16 strips of p-type electrodes was wire bonded to the input of a charge-sensitive preamplifier channel on a nearby die as shown in Fig. 3. Each preamplifier channel on the readout die is followed by a CR-RC shaping filter [7]. The shaping times can be varied by an externally supplied voltage. An integrating time of one microsecond was used for these measurements. The output of one channel of the preamplifier chip was sent via a coaxial cable to a variable-gain, NIM-format commercial amplifier. The signal from this amplifier was then split, with one part going to an oscilloscope, and the other to a peak-sensing analog-to-digital converter [8]. Its digital output values were then read out by a computer, stored on disk, and analyzed.

These data were taken at room temperature in a light-tight container. Both sources were effectively uncollimated and illuminated the entire area of the sensor under test. For the spectrum taken with a ^{55}Fe source, counts were acquired at a rate of 600 hertz. A ^{55}Fe spectrum acquired with the sensor reverse biased at 20 V is shown in Fig. 4. The noise determined with a pulse generator, with the detector still attached, had a full-width-at-half-maximum (FWHM) of 618 eV. A fit of two Gaussians with a common width, but two independent amplitudes and centroids, to the K_α/K_β merged peak gives a FWHM of 652 eV for the K_α peak. This fit is shown in Fig. 5.

Before the sensor was hooked up to the preamplifier, the leakage current from a single strip was less than 350 picoamperes when back biased at 20 V and at room temperature. Using a Peltier cooler, the temperature of the sensor and hence its bulk leakage currents were varied to study their influence on the resolution. When biased at 15 V, the FWHM for the ^{55}Mn K_α peak from the ^{55}Fe source varied from 634 eV at 25°C to 501 eV at 4°C. The peak width reported here differs from that in the

previous paragraph as it was recorded under slightly different conditions such as bias voltage, channel number, preamplifier bias currents, etc. These results demonstrate that leakage current was a significant, but not the dominant, contribution to the noise.

While not vital for this paper, it would be useful to verify that the measured noise, determined mostly by the total input capacitance, has the expected value. Preliminary results obtained by illuminating a sensor with a pulse of infrared light and measuring the decay time as the collected signal charge is bled through a 1 megohm resistor to ground, indicate that a single isolated electrode has a capacitance of around 200 femtofarads [5]. We expect that the most frequent uses of these sensors will be as pixel devices, with one amplifier per electrode, but for these measurements we tied all the electrodes in each row to a common bus to get an adequate counting rate without a large array of amplifiers. Such a row has a lower effective capacitance per electrode, since the neighbors on either side in the same row have the same voltage. To scale up the capacitance of a single electrode to that of a strip, we made the approximation that the capacitance is proportional to the number of nearest-neighbor electrodes whose voltage can vary relative to the strip voltage. Since a single electrode for which the capacitance was measured has six nearest neighbors, and a strip of fourteen electrodes with the same pattern and spacing has 32, we estimate that each strip would have a capacitance of approximately 1.1 pF, or about 1.2 pF including the wire bond.

One would expect this to lead to a FWHM of around 510 eV [7]. This value is similar to that measured when the sensor was cooled to 4°C. Thus the width of the ^{55}Mn K_α peak is dominated by the input capacitance of the sensor with the leakage current adding a substantial contribution.

Data were also taken with a ^{241}Am source with the sensor reverse biased at 25 V. The resulting spectrum is displayed in Fig. 6. In addition to the apparatus mentioned earlier, a passive attenuator with an attenuation of 8 dB was used between the preamplifier and the NIM amplifier. The spectrum was acquired at a rate of 10 Hz.

A fit to the Neptunium line at 14.3 KeV of a Gaussian with a linear background yielded a FWHM of 663 eV. The fitted function is given by (1)

$$n_{counts} = 212e^{-((529-b)^2/2\sigma^2)} + 28.9 - 0.43b \qquad (1)$$

where n_{counts} is the number of events per channel and b corresponds to the ADC bin number. The values of the numbers and σ, the standard deviation, are found from the best fit to the data. Fig. 7 shows a plot of this fit. The chi squared per degree of freedom was 1.15 for the channel range from 480 to 580. For the region centered on the peak and extending to 3σ on either side, from channel 498 to 560, the chi squared per degree of freedom was 1.03.

Since the primary orientation of the electric fields in a sensor with 3-D architecture is parallel to the top and bottom surfaces, signal charges are pulled directly toward collection electrodes and away from cell boundaries. This is in distinction to the situation found in typical planar-architecture sensors where only a small component of the electric field is parallel to the surface.

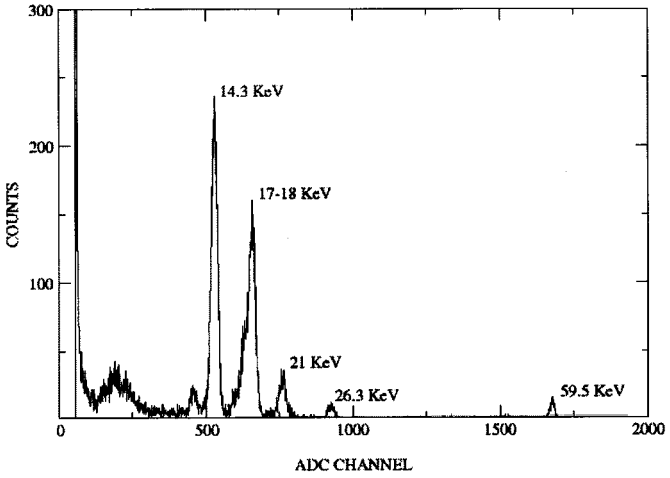

Fig. 6. Spectrum from an Americium-241 source.

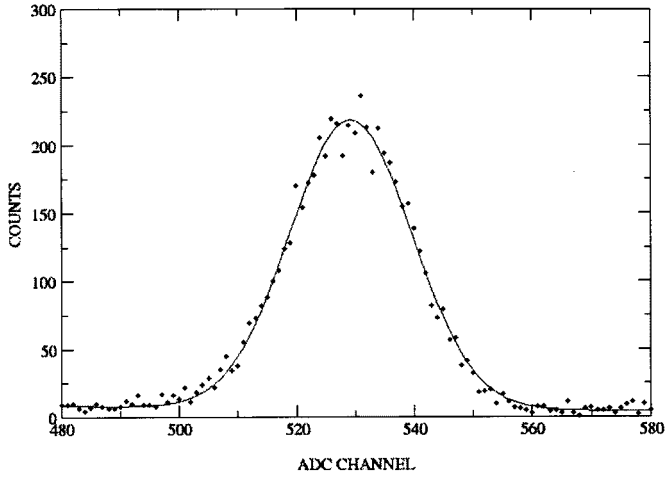

Fig. 7. Fit of a Gaussian with a linear background to the 14.3 KeV peak from the Americium spectrum of Fig. 6.

Therefore, one expects significantly less diffusion of the signal charge from one collection cell to an adjacent one in a 3-D architecture device. In addition, this sensor was significantly over biased, as its full depletion voltage is around 8 V, while it was biased at 25 V for the measurements reported here.

To study the actual degree of charge sharing with neighboring strips as well as any possible trapping of signal charges, a technique to quantify the asymmetry in the peak itself was used. To do this, the number of counts in a particular channel was subtracted from the number of counts predicted from the fit to the data, using the Gaussian with a linear background. This difference between the actual data and the fit was termed the residual. The number of residual counts in the low side of the peak between the three standard deviation point at channel 499 and the peak's center at channel 529 were summed. A similar summation was performed for the residual counts on the high side of the peak between channel 529 and 560. The summed residuals were found to be $-20(\pm 53)$ and $39(\pm 53)$ for the low and high half of the peak, respectively. As there were 5321 total counts in the peak after subtracting the linear background, these correspond to a deficit of 0.38% on the low side and a surplus of 0.73% on the high side. These results are statistically compatible with

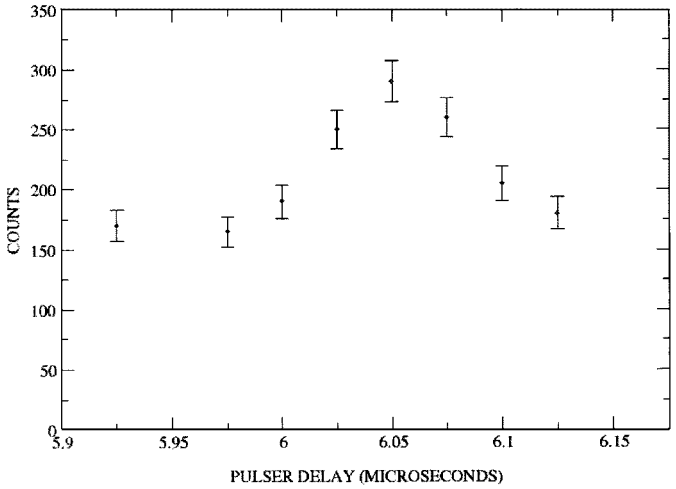

Fig. 8. Counting rate as a function of delay time between a scintillator and a 3-D sensor.

no shifting of counts from the high side of the peak to the low side, and of the opposite sign expected due to a partial loss of signal charge. While this result does not exclude a total charge loss due to trapping in the polycrystalline silicon electrodes or the single-crystal silicon, most charge-loss mechanisms would also produce partial pulse height signals that would have shifted counts from the high to low side of the peak.

III. Measurements with Beta Rays

The high radiation environment of the future LHC accelerator [9] presents challenges for the present silicon vertex detectors that may be helped by the 3-D architecture. We have used early prototypes of the ATLAS [10] silicon micro-strip front-end electronics and readout system, to detect beta particles from the device shown in Fig. 1. A simple telescope was constructed by placing the 3-D detector and electronics between a ^{106}Ru source and a scintillator connected to a photomultiplier tube used to trigger the readout system. The 3-D sensor used was the same as the one shown in Fig. 2 except that all of the p-type strips were shorted together with an aluminum trace. This resulted in a capacitance that is estimated to between 14 pF and 21 pF.

This single p-type channel of ganged 3-D sensors was bonded to the input of a charge sensitive LBIC [11] bipolar amplifier/comparator chip with a fast 20 ns shaping stage. A threshold was set on the LBIC comparator such that, for any signal above (below) 1 fC, a "1"(0) was passed to the output. This output bit was sampled at 40 MHz and stored in the circular 256 deep digital pipeline of a CDP128 chip [12]. An above-threshold signal from the photomultiplier tube produced a trigger to the data acquisition that could be delayed by a pulse generator. When the pulse generator delay was set so that the read/write pointer of the circular buffer had completed one cycle, the pipeline bit containing the triggered event was acquired. Fig. 8 shows the number of events for which the collected charge was greater than 1 fC, as a function of the pulse generator delay setting. 500 triggers were collected for each data point.

The clear excess of events seen when the pulse generator delay is in time (one complete buffer cycle), as compared to the out-of-time setting, is evidence of the detection of beta particles. The width of the signal peak was dominated by the output of the LBIC, which produces a 50 ns pulse, and by time-walk associated with the varying input pulse heights. The overall charge collection efficiency suffers from geometrical effects of our triggering system, and a measure of the charge deposition in the 3-D structure was not obtained.

IV. Conclusion

X rays of various energies have been detected by a microstrip sensor fabricated using a 3-D architecture. A FWHM for the Manganese K_α line of 652 eV was obtained. The width of the ^{55}Mn K_α peak is fully explained by the combined effects of the input capacitance and the leakage current. Hence signal charge collection problems in the sensor that would affect the observed resolution must be small. The symmetry of the 14 KeV Neptunium peak and the absence of anomalous peaks suggests fairly full charge collection with minimal diffusion of signal charge between strips. Beta rays were also observed in coincidence with a scintillation detector.

Acknowledgment

The authors would like to thank J. Segal, C. Storment, and J. McVittie for providing valuable information and advice throughout this project; A. Partridge, who allowed use of the wafer bonding apparatus; the staff of the Stanford Nanofabrication Facility who provided help in countless ways; and J. Plummer and H. Yamamoto for their interest and support. They also appreciate the wire-bonding and mechanical work performed by G. Zizka, B. Rowe, and A. Webster. They have received vital help in the form of computer support and office space from the Stanford Linear Accelerator Center and the Lawrence Berkeley Laboratory.

References

[1] S. Parker, C. Kenney, and J. Segal, "3-D—A proposed new architecture for solid-state radiation detectors," *Nucl. Instrum. Meth.*, vol. A 395, pp. 328–343, Aug. 1997.

[2] C. Kenney, S. Parker, J. Segal, and C. Storment, "Comparison of 3-D and planar silicon detectors," in *Proc. 9th Meeting Division Particles Fields American Physical Society*, Minneapolis, MN, Aug. 11–15, 1996, pp. 1342–1345.

[3] ——, "Silicon detectors with 3-D electrode arrays: Fabrication and initial test results," *IEEE Trans. Nucl. Sci.*, vol. 46, pp. 1224–1236, Aug. 1999.

[4] G. Lindstrom, M. Moll, and E. Fretwurst, "Radiation hardness of silicon detectors—A challenge from high-energy physics," *Nucl. Instrum. Meth.*, vol. A 426, pp. 1–15, 1999.

[5] S. Parker and C. Kenney, "Performance of 3-D architecture, silicon sensors after intense proton irradiation," University of Hawaii, Preprint UH-511-959-00.

[6] A. Meikle, R. Bates, K. Mathieson, V. O'Shea, and K. Smith, "3-D GaAs radiation detectors," in 5th Int. Conf. Position-Sensitive Detectors, London, U.K., 1999.

[7] B. Ludewigt, J. Jaklevic, I. Kipnis, C. Rossington, and H. Spieler, "A high rate, low noise, x-ray silicon strip detector system," *IEEE Trans. Nucl. Sci.*, vol. 41, pp. 1037–1041, Aug. 1994.

[8] M. R. Maier, B. Ludewigt, C. Rossington, H. Yaver, and J. Zaninovich, "A sixteen channel peak sensing ADC for singles spectra in FERA format," *IEEE Trans. Nucl. Sci.*, vol. 43, pp. 1680–1682, June 1996.

[9] "ATLAS technical proposal for a general purpose PP experiment at the LHC," Rep. CERN/LHCC/94-43, 1994.
[10] "ATLAS TDR 5, inner detector technical design report,", CERN/LHCC/97-17, vol. II, 1997.
[11] E. Spencer *et al.*, "A fast shaping low power amplifier-comparator integrated circuit for silicon strip detectors," *IEEE Trans. Nucl. Sci.*, vol. 42, pp. 796–802, Aug. 1995.
[12] J. DeWitt, "A pipeline and bus interface chip for silicon strip detector readout," in *IEEE Nuclear Science Symp.*, San Francisco, CA, Nov. 1993, SCIPP 93/37.